ACES Asian Chemical Editorial Society

doi.org/10.1002/cnma.202200093

CHEMNANOMAT
Research Article

www.chemnanomat.org

Water Remediation from Pollutant Agents by the Use of an Environmentally Friendly Supramolecular Hydrogel

Demetra Giuri[+], Simone D'Agostino[+], Paolo Ravarino, Davide Faccio, Giuseppe Falini,* and Claudia Tomasini*[a]

Abstract: The removal of Diclofenac sodium from waste waters has a high relevance since it belongs to the therapeutic group most commonly found in wastes. An aromatic-free and low-impact technology that efficiently entraps aqueous pollutants is highly desirable. We synthesised two Boc-protected and aromatic-free tripeptides (Boc-L-Ala-Aib-L-Val-OH and Boc-L-Val-Aib-L-Val-OH) and studied their ability to form gels with mixtures of water and alcohols, such as methanol, ethanol and 2-propanol. Boc-L-Ala-Aib-L-Val-OH forms a strong hydrogel in 2-propanol/water mixtures able to trap up to 97.8% of Eosin Y model molecule and up to 92.0% of Diclofenac sodium from aqueous solutions. The hydrogel is also thixotropic, thermoreversible and biocompatible. This outcome is very encouraging and paves the way to a new approach for developing new materials using aromatic-free hydrogels, useful for water remediation.

Introduction

Due to the ease of modifications, short peptides are highly attractive scaffolds for supramolecular assemblies.[1,2] Several short peptides containing aromatic amino acids are able to form self-assembled materials as fibers, layers and gels, as the aromatic ring is crucial to build the hierarchical processes that form the materials through a bottom-up approach.[3,4] For example, phenylalanine (Phe),[5] tyrosine (Tyr),[6] Dopa[7] produce a plethora of peptides and proteins able to form self-assembled biomaterials with unique structural features.

The most popular dipeptide that has been used for this purpose is Phe-Phe, as it is a key fragment from the Amyloid peptide Aβ-42 involved in Alzheimer's disease.[8] It forms robust nanotubular morphologies and has emerging uses as highly ordered biomaterials with applications in various fields of biotechnology and nanomedicine.[9]

Short peptides containing aromatic rings have also been used as low-molecular-weight gelators (LMWG),[10,11] that are special group of organic molecules that have a molecular weight $<1{,}000$ Da and self-assembles in solvents to form long, fibrous structures,[12] through a combination of non-covalent interactions like H-bonding, π-π stacking, donor-acceptor interactions, metal coordination, and van der Waals interactions.[13,14] These fibres often form three-dimensional networks that immobilise water or the organic solvent, thus behaving as a supramolecular cross-linked polymer in the hydrogel formation. Since these networks involve weak interactions, the gel-to-sol transition is facile (and usually rapid) as compared to polymeric gelators, so they can be readily transformed to a fluid (sol) by heating and are generally thermally reversible. For this reason, the presence of aromatic rings is often crucial to form a stable self-assembled structure.[15] The drawback of this choice is that aromatic rings are not easily biodegradable, so the use of aromatic-free gelators for the formation of supramolecular materials is highly desirable.

Supramolecular gels[16,17] have several applications including sensing of biomolecules and ions,[18–20] light-harvesting systems,[21] catalysis,[22] optoelectronic devices,[23,24] tissue engineering,[25] targeted drug delivery,[26] crystal growth,[27] dyes and pollutant removal[28–31] and degradation[32] and may be implied as injectable gels.[33] We want to show in this paper how an aromatic-free supramolecular gel may be efficiently used for water remediation. It is worth mentioning that no nanomaterial (graphene derivatives, nanotubes, nanoparticles) was introduced in the system,[34–37] to avoid any release of the nanomaterial in water. This material is cheap, readily available and easily biodegradable and opens the way to the production of environmentally friendly materials that may be applied to water remediation. Water has always been one of the most essential entities for the survival of living systems almost since the evolution of life form. It is pertinent to study water systems in respect of enhancing the quality of water as it can be a significant source affecting the living systems directly or indirectly. Nowadays, the increased level of water consumption and correspondingly high levels of pollution have generated a prominent need for managing the water quality by maintaining safe levels for the water to be used in specific applications. In this respect, water remediation methods have taken a forward thrust[38–41] to increase the water quality of potable water as well as that of industrial grade water in to prevent contamination of

[a] Dr. D. Giuri,[+] Dr. S. D'Agostino,[+] P. Ravarino, D. Faccio, Prof. G. Falini, Prof. C. Tomasini
Dipartimento di Chimica Giacomo Ciamician
Università di Bologna
Via Selmi, 2 – 40126 Bologna (Italy)
E-mail: claudia.tomasini@unibo.it
giuseppe.falini@unibo.it

[+] These authors contributed equally.

Supporting information for this article is available on the WWW under https://doi.org/10.1002/cnma.202200093

natural water resources due to the discharge of industrial effluents.

Results and Discussion

Hydrogels preparation

The aim of this work is to prepare biodegradable, aromatic-free hydrogels and to apply them to water remediation from polluting diclofenac. Thus, we prepared the two Boc-protected tripeptides Boc-L-Ala-Aib-L-Val-OH **A** and Boc-L-Val-Aib-L-Val-OH **B** (Figure 1), both containing the aminoisobutiric acid in the central position, and we tested their attitude to form hydrogels under several conditions. The two tripeptides **A** and **B** were prepared by traditional liquid phase synthesis with excellent yield from cheap starting materials, and they were both easily available in multigram scale.

Then, we attempted to form hydrogels under several conditions. A very promising approach is to use mixtures of water and short alcohols as methanol, ethanol and 2-propanol, because all the alcohols readily mix with water and solubilize both **A** and **B**, while water acts as non-solvent. To find the best condition to form strong and self-supporting hydrogels, we tested several mixtures of water and the three alcohols (Table S1). In any case, we used a 1% w/w gelator concentration. Good results have been obtained only with gelator **A** with 3:7 mixtures of EtOH/H_2O and iPrOH/H_2O (samples **4** and **7**), as the ratio between water and the alcohol was crucial to obtain a self-supporting gel. In contrast, none MeOH/H_2O mixture produces a self-supporting gel but only partial gels. In Figure 2 the outcome of the gelation processes listed in Table S1 are shown.

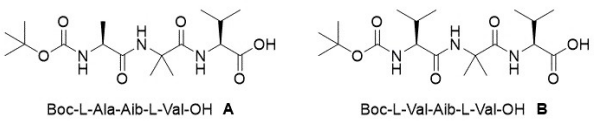

Figure 1. Chemical structure of the two tripeptides **A** and **B**.

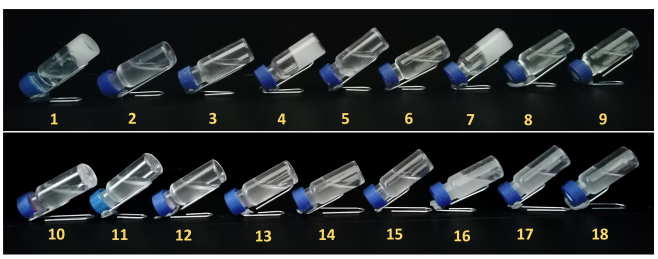

Figure 2. Photographs of attempts for the formation of hydrogels with tripeptide **A** (top) and tripeptide **B** (down) under the conditions listed in Table S1. Only tripeptide **A** behaves as gelator and forms gels with 3:7 mixtures of EtOH/H_2O and iPrOH/H_2O.

Hydrogel Characterization

Much to our surprise, only **A** is able to form hydrogels, while **B** has a strong tendency to form crystals under several conditions. This different behaviour is probably ascribed to the replacement of an Ala unit with the Val unit. To shed light on the organization in gel fibers and to get insights into the relationship between the chemical structure of the two Boc-protected tripeptides **A** and **B** and their gelation properties, we underpinned an XRD crystallographic characterization as well.

Crystals of the non-gelling **B** suitable for XRD diffraction were readily obtained from slow evaporation of an ethanolic solution, whereas for the gelling compound **A** crystallization resulted quite difficult and only very thin and highly interwoven needle-like crystals grew from a water/acetonitrile mixture (1:9). Structural XRD analysis revealed that **A** and **B** crystallize in the chiral space groups triclinic-P1 and orthorhombic-$P2_12_12_1$ respectively (see Table S2 for details). In the case of **A**, we could not fully model the structure because of the severe crystallographic disorder affecting one out of the two Boc-Ala-Aib-Val-OH molecules comprising the asymmetric unit; on the other hand, the second molecule was easily located and successfully refined. In each case, the packing includes a crystallization solvent molecule. H_2O for **A** and EtOH for **B**. As the result of the weak and distorted intramolecular hydrogen bond between the Boc-carbonyl and the NH from the Val-residue of the O-terminus [$N_{N-H}\cdots O_{C=O} = 3.51(2)$ Å and 3.84(1) Å for **A** and **B**, respectively] (Figure 3), and analogously to other reported Boc-protected tripeptides[42,43] both compounds adopt a similar folded conformation (Figure S1 and Table S3 for backbone torsion angles), corresponding to a distorted β-turn structure.[44,45]

Despite the very similar molecular conformations, **A** and **B** show quite different crystal packings. This could directly consequence the different *N*-terminus residue and crystallization solvents, which play an active role in determining the solid-state arrangements. In crystalline **A**, water molecules bridge the adjacent peptide molecules through hydrogen bonds with the Val- and Ala-residues [$O_{O-H}\cdots O_w = 2.55(1)$ Å, and $O_w\cdots O_{C=O} = 2.84(2)$ Å, respectively] to form chains which are further stabilized by additional interactions between the NH and carbonyl belonging to the same residues [$N_{N-H}\cdots O_{C=O} = 2.94(1)$ Å]. Water molecules also link adjacent chains via interactions with the C=O from another Val-residue [$O_w\cdots O_{C=O} = 2.81(1)$ Å], whereas the Aib-residues form hydrogen bonds

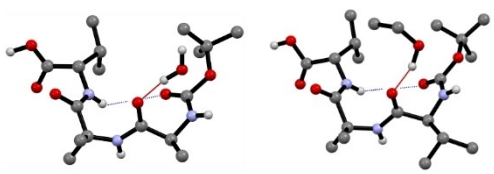

Figure 3. Molecular structure of crystalline **A** (left) and **B** (right) showing the intramolecular hydrogen bond (blue-line) responsible for the folded conformations, and the intermolecular hydrogen bond with the respective crystallization solvents (red-line). H_{CH} atoms omitted for clarity

among them [$N_{N-H}\cdots O_{C=O}$ = 2.92(1) Å], the overall result is the formation of a complex 2D net, as depicted in Figure 4.

In crystalline **B**, EtOH engages intermolecular hydrogen-bonding interactions with the Val-residues from the N- and O-termini [$O_{O-H}\cdots O_{C=O}$ = 2.66(1) Å and 2.62(1) Å, respectively] and belonging to adjacent Boc-Val-Aib-Val-OH molecules (Figures 3a and 5a). The two Val-residues also form direct hydrogen bonds [$N_{N-H}\cdots O_{C=O}$ = 3.02(1) Å], leading to a 1D chain running parallel to the a-axis (Figure 4a). Other hydrogen bonding interactions are detected among the Aib-residues [$N_{N-H}\cdots O_{C=O}$ = 3.02(1) Å] and are responsible for forming 1D chains that run along the b-axis (Figure 5b).

The phase purity of **A** and **B** was established by comparison of their observed and simulated powder X-ray diffraction. The resulting good match between the two patterns is shown in Figure S2 for both compounds.

Then the mechanical properties of the two hydrogels **4** and **7** obtained by self-assembly of **A** were studied. Neither sample showed recovery when harshly shaken and left to rest. Following a different technique to completely dissolve the fibres network, we placed the gels inside a water bath and increased the temperature up to 60 °C. This process resulted in the dissolution of the gel with the formation of a clear solution, that was left to rest afterwards at 25 °C for 4 hours. Sample **4** after heating reformed only partially to produce the partial gel **4_H**, while gel **7_H** reformed almost completely (Figure 6).[46] Since gel **7** showed increased mechanical properties and better recovery compared to gel **4**, we prepared a new gel (**19**) following the same procedure above described and using **A** in 2% concentration. The hydrogel **19** is a strong material, is perfectly thermoreversible after heating at 60 °C and cooling at 25 °C (**19_H**), meaning that if the network is completely dissolved the gel can be reformed with the same properties. Moreover, even after hard shake, the gel is reformed (**19_S**).

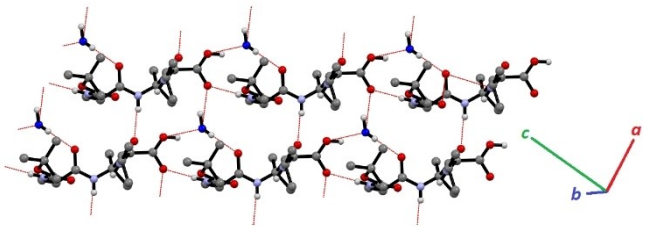

Figure 4. The complex 2D net of hydrogen bonding interactions detected in crystalline **A**. Ow-atoms in blue and HCH-atoms omitted for clarity.

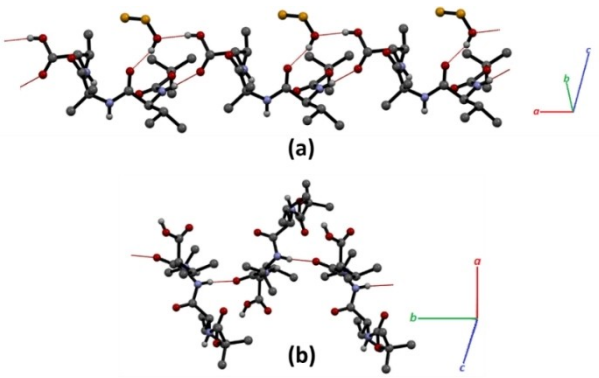

Figure 5. (a) Hydrogen bonds between the EtOH and the Val-residues of the C- and N-termini, and (b) hydrogen bonds between the Aib-residues in crystalline **B**. C_{EtOH}-atoms in orange and H_{CH}-atoms omitted for clarity.

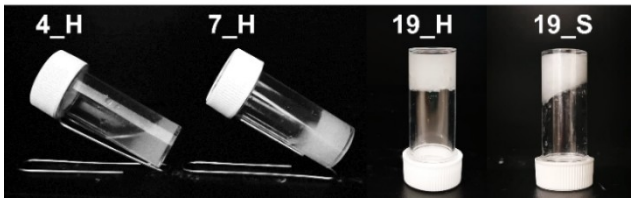

Figure 6. Pictures of the samples reformed after the heating/cooling process (identified as "**_H**") or after shaking (identified as "**_S**"). **4_H**: gelator **A** in 1% concentration in 1:2 ratio EtOH/H_2O; **7_H**: gelator **A** in 1% concentration in 1:2 ratio iPrOH/H_2O; **19_H**: gelator **A** in 2% concentration in 1:2 ratio iPrOH/H_2O. **19_S**: gelator **A** in 2% concentration in 1:2 ratio iPrOH/H_2O.

The mechanical properties of the gels **4**, **7** and **19** were analysed with a rheometer and the results are reported in Figure 7 and in Table S4. In any case, the storage modulus G′ is higher than the loss modulus G″, as expected for gels. The amplitude sweeps for gels **4** and **7** are almost superimposable, with G′ values in the order of 10^2 kPa, while gel **19** showed better results, with a G′ value in the order of 10^3 kPa. Although **4** and **7** behave similarly, the thixotropy test provides a better outcome with gel **7**, as disclosed in the shaking and melting experiments. Consistently, gel **19** showed excellent thixotropy properties with complete recovery of the mechanical properties (Figure 6). The mechanical properties of the three samples **4**, **7** and **19** were analysed again with the rheometer after the heating and cooling process. The new amplitude sweeps (Figure 7) show similar behaviour to those before the heating and cooling process, although for gel **4** some water outside the gel was observed and partially alters the outcome.

The morphological analysis of gels **4** (Figure 8) and **7** was performed on both wet samples, using an optical microscope, and dry samples, using Scanning Electron Microscopy (SEM). Wet samples show similar structures, with long thin and flexible fibers randomly aligned. SEM analysis, instead, highlights differences in aspect ratio and texture in the fibres making the xerogels from sample **4** and sample **7** (Figure 9). Both samples form fibers that can reach a maximum length of about 0.5 mm (Figure 9 a and b insets), but with a maximum width of about 10 mm and about 5 mm for sample **4** and **7**, respectively. Sample **4** shows a laminar structure (Fig. 9c) and well-defined crystalline faces. In this sample bundles of fibers are observed, but the fibers are not branched (Figure 9a and c). Differently, sample **7** shows a poor crystalline aspect having fibers with rounded edges and highly branched and interconnected (Figure 9b and d).

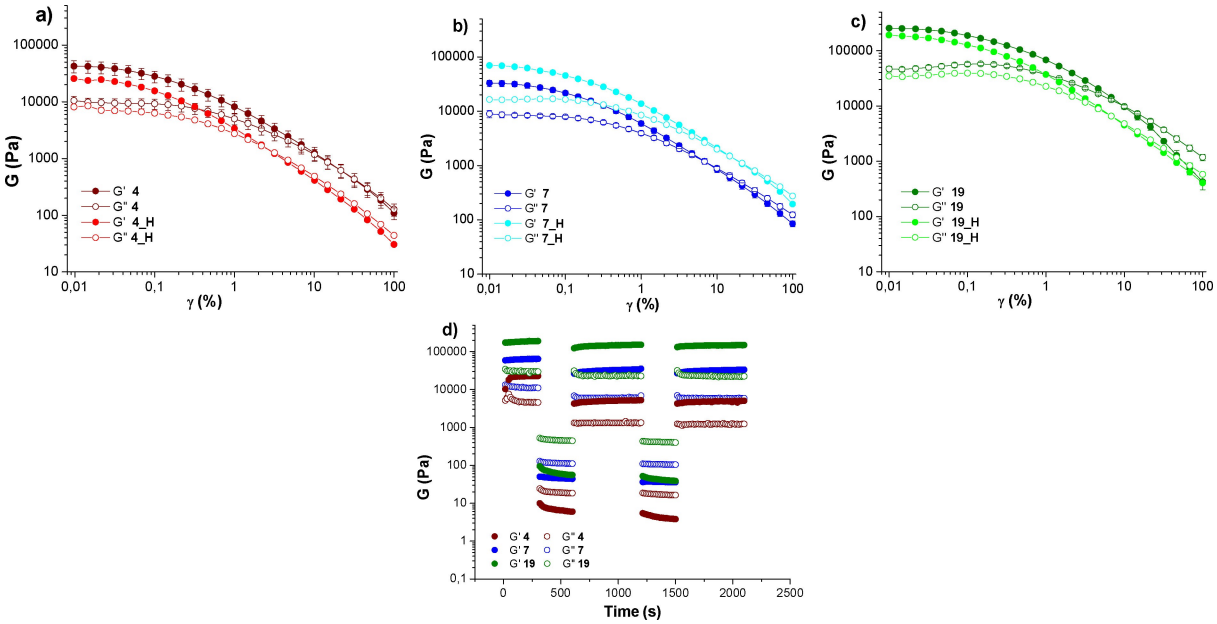

Figure 7. (a) Superimposition of the amplitude sweeps of the samples **4** (gelator **A** in 1% concentration in 1 : 2 ratio EtOH/H_2O) and **4_H** (gelator **A** in 1% concentration in 1 : 2 ratio EtOH/H_2O after heating/cooling process); (b) superimposition of the amplitude sweeps of the samples **7** (gelator **A** in 1% concentration in 1 : 2 ratio iPrOH/H_2O) and **7_H** (gelator **A** in 1% concentration in 1 : 2 ratio iPrOH/H_2O after heating/cooling process); (c) superimposition of the amplitude sweeps of the samples **19** (gelator **A** in 1% concentration in 1 : 2 ratio iPrOH/H_2O) and **19_H** (gelator **A** in 2% concentration in 1 : 2 ratio iPrOH/H_2O after heating/cooling process); (d) superimposition of the step-strain experiments of samples **4**, **7** and **19**.

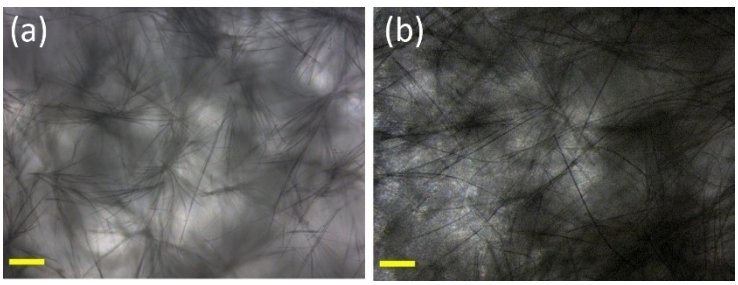

Figure 8. (a) Optical microscope images of wet hydrogels **4** (gelator **A** in 1% concentration in 1 : 2 ratio EtOH/H_2O); (b) Optical microscope images of wet hydrogels **7** (gelator **A** in 1% concentration in 1 : 2 ratio iPrOH/H_2O). Scale bar: 100 μm.

Hydrogels Applications: Pollutant Absorption

In our previous works we demonstrated the possibility to efficiently remove aromatic pollutants from water using LMWGs containing several aromatic rings.[28,29] In this study, the possibility to remove aromatic pollutants from water using the aromatic-free hydrogels **7** and **19** was tested. We prepared some samples of both hydrogels to check the relation between gel strength and its absorption capability. Eosine Y (EY, 0.016 mg/mL) was chosen as model dye pollutant, as we also used it in a previous work,[28] while Diclofenac sodium (DIC, 0.02 mg/mL) was chosen as drug, since it belongs to the therapeutic group most commonly found in water.[47–51] The pollutant solutions were eluted through a 2 mL gel column, that was prepared directly into a 10 mL syringe (Figure 10). For both pollutants, a calibration curve was built (Figures S3 and S4).

Eosin Y was chosen as model molecule because its absorption may be easily quantified using a Uv-vis spectrophotometer, through the comparison of the results with a calibration curve. In Table 1 the results are reported for both gels **7** and **19**. As we could foresee, the increased strength of **19** increases the pollutant absorption, under the same conditions (entry 1 *versus* 3 and entry 2 *versus* 4), reaching an excellent

Table 1. Absorption of Eosine Y (EY) in hydrogels **7** and **19** under different conditions, repeated in triplicate.

Entry	Hydrogel	Gelator [μmol]	EY [μmol]	Solution [mL]	Detained EY [%]
1	7	53.6	0.12	5	80.8 ± 0.5
2	7	53.6	0.24	10	65.4 ± 6.0
3	19	107.0	0.12	5	97.8 ± 0.9
4	19	107.0	0.24	10	91.1 ± 3.2

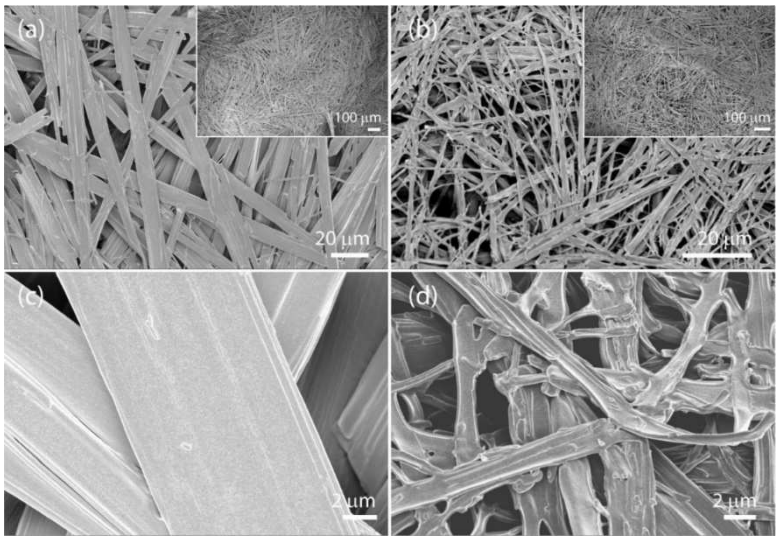

Figure 9. Scanning electron microscope (SEM) images of xerogels **4** (gelator **A** in 1% concentration in 1:2 ratio EtOH/H_2O) (a and c) and **7** (gelator **A** in 1% concentration in 1:2 ratio iPrOH/H_2O) (b and d). The insets show low magnification images.

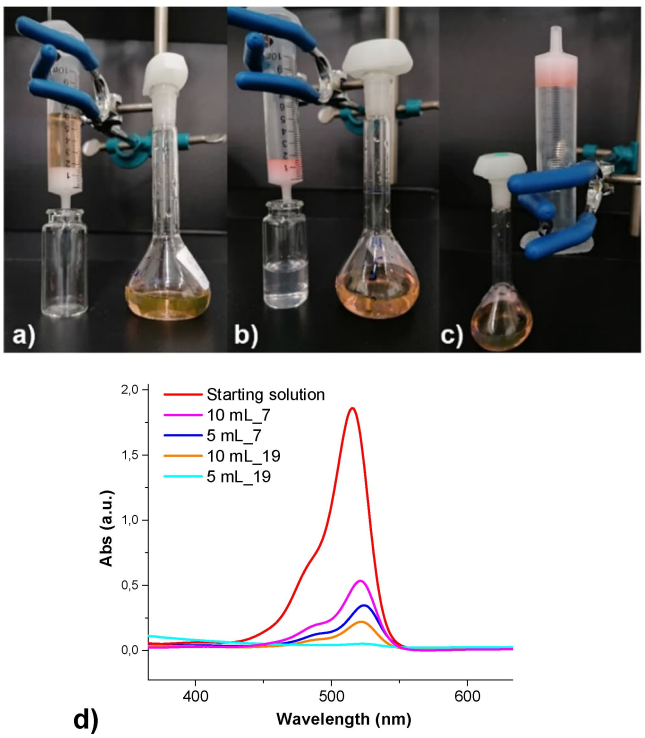

Figure 10. (a) Absorption test of an EY solution (5 mL) on gel **19** (gelator **A** in 2% concentration in 1:2 ratio iPrOH/H_2O) at the beginning of the process. (b) Absorption test of an EY solution (5 mL) on gel **19** at the end of the process: the eluted solution is colorless. (c) Inversion of the gel sample after the process. (d) Absorption spectrum of the starting solution of EY, compared with the collected solutions after elution under the conditions of entries 1–4.

result of 97% detained EY when hydrogel **19** is used. At the end of the absorption experiment, all gels were stable enough to be inverted without flowing (Figure 10c). The fibrous structure of the gel was preserved after the test and even highlighted thanks to the presence of the dye, as it is shown by the epifluorescence image (Figure S7).

The absorption ability of hydrogels **7** and **19** was also tested for DIC, as reported in Table 2. Unfortunately, in these cases the absorption ability of both hydrogels **7** and **19** is lower than for EY, although using an increased gel concentration (**19**) affords better results. When the amount of polluted solution is increased (from 5 to 10 mL), we can observe a decreased ability of pollutant absorption. Curiously, when the same pollutant amount of entry 4 is dissolved in 5 mL (doubling its concentration), excellent results are obtained with the absorption of 88.6% of the original DIC amount. This means that a key point in the absorption test for these materials is the amount of solution eluted through the hydrogel, that should not exceed too much the hydrogel volume.

Conclusion

In this paper we have shown that it is possible to use the Boc-protected and aromatic-free short peptides Boc-L-Ala-Aib-L-Val-OH to prepare supramolecular gels able to trap polluting molecules as Diclofenac sodium. The removal of this polluting molecule in waste waters has a high relevance since it belongs to the therapeutic group most commonly found in water. The

Table 2. Absorption of Diclofenac (DIC) in hydrogels **7** and **19** under different conditions, repeated in triplicate.

Entry	Hydrogel	Gelator [µmol]	DIC [µmol]	Solution [mL]	Detained DIC [%]
1	7	53.6	0.32	5	44.7 ± 3.2
2	7	53.6	0.65	10	25.6 ± 3.3
3	19	107.0	0.32	5	83.8 ± 0.4
4	19	107.0	0.65	10	51.0 ± 4.7
5	19	107.0	0.62	5	92.0 ± 3.0

study of the most suitable tripeptide was crucial to obtain an efficient soft material for water remediation. This outcome was achieved by a careful study of the most suitable gelator and gelation conditions. We analysed the crystallographic structure of the peptide, the rheological properties of the different hydrogel samples and the morphology of self-assembled fibres. As a consequence of our careful screening combining all these techniques, we envisaged a strong, self-supporting hydrogel containing only 2% w/w ratio of tripeptide that is able to trap up to 97.8% of the Eosin Y model molecule and up to 92.0% of Diclofenac sodium. The hydrogel is also thixotropic, thermoreversible and biocompatible.

This remediation method is low impact, very fast and cheap, as the trapping system may be easily prepared in any condition with readily available reagents.

The gelator degradation has no drawbacks, as the tripeptides are fully biocompatible. Moreover, the lack of any aromatic ring further reduces the environmental impact.

Last but not least, the use of small peptides to promote the hydrogel formation is alternative to the use of polymers, that often have a reduced biodegradability. Moreover, these hydrogels are more versatile for several applications, as the polymeric gels are seldom thixotropic.

This outcome is very encouraging and paves the way to a new approach for developing new materials for water remediation using aromatic-free hydrogels.

Experimental Section

Preparation of Boc-L-Ala-Aib-L-Val-OH A and Boc-L-Val-Aib-L-Val-OH B. All reactions were carried out in dried glassware and using dry solvents. The melting points of the compounds were determined in open capillaries and are uncorrected. High quality infrared spectra (64 scans) were obtained at 2 cm^{-1} resolution with an ATR-IR Bruker (Billerica, US, MA) Alpha System spectrometer. All compounds were dried in vacuo and all the sample preparations were performed in a nitrogen atmosphere. NMR spectra were recorded with a Varian (Palo Alto, US, CA) Inova 400 spectrometer at 400 MHz (^{1}H NMR) and at 100 MHz (^{13}C NMR). Chemical shifts are reported in δ values relative to the solvent peak. HPLC-MS analysis was carried out with an HP1100 liquid chromatograph coupled to an electrospray ionization mass spectrometer (LC-SI-MS), using a Phenomenex Gemini C18- - 3 μ – 110 Å column, H_2O/CH_3CN with 0.2% formic acid as acid solvent at 40 °C (positive ion mode, mz = 50–2000, fragmentor 70 V).

Gel Preparation Concentration. To prepare the 1% w/w gels, 10 mg of compound **A** or **B** were weighted in a 2 mL vial. Then the organic solvent (ethanol, methanol or 2-propanol, for the amount see Table 1) was added, and the mixture was sonicated until complete dissolution (10 minutes) in an *Elmasonic S* ultrasound sonicator (37 kHz). The required amount of milliQ water to reach the final volume of 1 mL (see Table 1) was then added to the solution. All samples were left to stand quiescently for 16 h before the analyses. The same procedure was followed to prepare the 2% w/w gels, using 20 mg of compound **A** instead of 10 mg.

Preparation of 4_H, 7_H, 19_H and 19_S. After the preparation of gels **4**, **7** and **19** we tested the recovery properties of the materials after break. We tried two different methods to break the gels: shaking (the sample were named with the number of the corresponding gel and the addition of **_S**) or heating up to 60 °C (the sample were named with the number of the corresponding gel and the addition of **_H**). With the first method the gel was manually shaken, obtaining a solution with fibers, and left to rest overnight. With the second method the fibres network was completely dissolved by heating: the gels were placed inside a water bath and the temperature increased up to 60 °C. This process resulted in the dissolution of the gel with the formation of a clear solution, that was left to rest afterwards at 25 °C for 4 hours.

Gel Preparation Concentration in Syringes for Water Remediation. For the preparation of the gels at 1% w/w concentration in syringe, 2 mL of gel column were prepared into a 10 mL syringe, sealed at the bottom with parafilm. The gelator powder (20 mg) was weighted into a vial and sonicated with the correct volume of organic solvent. When a clear solution was obtained, it was transferred into the syringe, and water was added directly into the syringe to form the gel. The ratio between organic solvent and water were exactly the same reported in Table 1.

For the preparation of the gels at 2% w/w concentration in syringe, 2 mL of gel column were prepared into a 10 mL syringe, sealed at the bottom with parafilm. The gelator powder (40 mg) was weighted into a vial and dissolved with the correct volume of organic solvent by simple manual agitation, until a clear solution is formed. The sonication in this case should be avoided because it causes the formation of a gel even before the addition of water, due to the high concentration of gelator. When the gelator is dissolved, water was added directly inside the vial and then the solution was immediately transferred into the syringe.

Crystal Structure Determination. Single-crystal data for the Boc-protected tripeptides **A** and **B** were collected at RT on an Oxford XCalibur S CCD diffractometer equipped with a graphite monochromator (Mo-K_α radiation, λ = 0.71073 Å). All samples were of poor quality, invariably obtained as small needles and weakly diffracting. Additionally, crystals of **A** suffered heavily twinning, for the best sample found and analyzed, two twin unit cells were indexed, and the reflection data were integrated with the default configuration for twinned crystals of the *CrysAlisPro* software. Subsequent structure solution and refinement were performed using the HKLF4 file containing nonoverlapped reflections. The structures were solved by intrinsic phasing with SHELXT[52] and refined on F^2 by full-matrix least squares refinement with SHELXL[53] implemented in the Olex2 software.[54] All non-hydrogen atoms were refined anisotropically and applying the rigid-body RIGU restraint.[55] H atoms for all compounds were directly located or added in calculated positions and refined riding on their respective atoms. Data collection and refinement details are listed in Table S1. In crystalline **A**, one molecule could not be unambiguously determined because of severe disorder; therefore, its contribution to the calculated structure factors was removed by using the Solvent Mask function implemented in the Olex2 software.[54] The Mercury[56] program was used to calculate intermolecular interactions and for molecular graphics. Crystal data can be obtained free of charge via www.ccdc.cam.ac.uk/conts/retrieving.html (or from the Cambridge Crystallographic Data Centre, 12 Union Road, Cambridge CB21EZ, UK; fax: (+44)1223-336-033; or e-mail: deposit@ccdc.cam.ac.uk); CCDC numbers 2117629 (A) and 2117625 (B).

Powder Diffraction Measurements. For phase identification X-ray powder diffraction experiments, diffractograms were recorded on a PANalytical X'Pert Pro automated diffractometer equipped with an X'Celerator detector in Bragg-Brentano geometry, using Cu-Kα radiation (λ = 1.5418 Å) without monochromator in the 2θ range between 5° and 40° (continuous scan mode, step size 0.0167°, counting time 19.685 seconds, Soller slit 0.04 rad, antiscatter slit 1/2, divergence slit 1/4, 40 mA···40 kV). The program Mercury[56] was used for the calculation of the X-ray powder patterns on the basis

of single-crystal data collected in this work. The identity between the polycrystalline materials samples and the structures obtained by single crystals was always verified by comparing calculated and experimental powder diffraction patterns.

Rheology Test. All rheological measurements were performed using an Anton Paar (Graz, Austria) MCR102 rheometer. The gels were prepared as described and tested directly in the Thermo Fisher Scientific (Waltham, MA, US) Sterilin cup, which fits in the rheometer. A vane and cup measuring system was used, setting a gap of 2.1 mm. Oscillatory amplitude sweep experiments (γ: 0.01–100%) were performed at 23 °C using a constant angular frequency of 10 rad/s, after 16 h from the addition of water, to allow a complete gel formation. Also step strain experiments were performed on hydrogels after 16 h, subjecting the sample to consecutive deformation and recovery steps. The first step (rest conditions) was performed at a constant strain $\gamma = 0.05\%$ (within the LVE region) and at a fixed frequency of $\omega = 10\ rad\ s^{-1}$ for a period of 300 s. The deformation step was performed applying a constant strain of $\gamma = 100\%$, (above the LVE region) for a period of 300 s. The recovery cycle was performed with the same conditions of the first step for a period of 400 s. Deformation and recovery steps were repeated two times.

Optical Microscope Images. The optical microscope images were recorded using a Nikon (Minato, Japan) 13 ECLIPSE Ti2 Inverted Research Microscope with a 10× magnifier. A piece of the gel sample prepared in the Sterilin cups was analysed while wet and after complete drying. The images after dye absorption were taken in epifluorescence mode, using a fluorescent filter cube V-2 A and an excitation LED ($\lambda = 395$ nm).

Scanning Electron Microscopy. Scanning electron micrographs were recorded on carbon coated samples using a Zeiss LEO 1530.

Supplementary materials

Supplementary material associated with this article can be found, in the online version, at doi: XXX: Synthesis and characterization of compounds **A** and **B**; ^{1}H NMR, ^{13}C NMR and IR spectra of compounds **A** and **B**; Crystal data and refinement details; Overlay of the molecular structures of crystalline **A** and **B**; Selected backbone torsion angles for **A** and **B**; XRD diffraction patterns for **A** and **B**; Calibration curve of Eosine Y; Calibration curve of Diclofenac sodium; Microscope image of a sample of 7 after dye absorption.

Acknowledgements

We gratefully acknowledge the University of Bologna, the Ministero dell'Università e della Ricerca (PRIN 2017 project 2017CR5WCH) and the Fondazione CarisBo for the funding of the project #18668 Tecnologie avanzate per il controllo e lo sviluppo di molecole innovative per la salute. Open Access Funding provided by Universita degli Studi di Bologna within the CRUI-CARE Agreement.

Conflict of Interest

The authors declare no conflict of interest.

Data Availability Statement

The data that support the findings of this study are available in the supplementary material of this article.

Keywords: aromatic-free peptides · crystals · hydrogels · water remediation

[1] P. Chakraborty, E. Gazit, *ChemNanoMat* **2018**, *4*, 730–740.
[2] P. Makam, E. Gazit, *Chem. Soc. Rev.* **2018**, *47*, 3406–3420.
[3] E. De Santis, M. G. Ryadnov, *Chem. Soc. Rev.* **2015**, *44*, 8288–8300.
[4] R. De La Rica, H. Matsui, *Chem. Soc. Rev.* **2010**, *39*, 3499–3509.
[5] T. Das, M. Häring, D. Haldar, D. Díaz Díaz, *Biomater. Sci.* **2018**, *6*, 38–59.
[6] J. Lee, M. Ju, O. H. Cho, Y. Kim, K. T. Nam, *Adv. Sci.* **2019**, *6*, DOI 10.1002/advs.201801255.
[7] D. Giuri, P. Ravarino, C. Tomasini, *Org. Biomol. Chem.* **2021**, *19*, 4622–4636.
[8] M. Reches, E. Gazit, *Science* **2003**, *300*, 625–627.
[9] S. Marchesan, A. V. Vargiu, K. E. Styan, *Molecules* **2015**, *20*, 19775–19788.
[10] J. Raeburn, C. Mendoza-Cuenca, B. N. Cattoz, M. a. Little, A. E. Terry, A. Zamith Cardoso, P. C. Griffiths, D. J. Adams, *Soft Matter* **2015**, *11*, 927–935.
[11] P. R. A. Chivers, D. K. Smith, *Nat. Rev. Mater.* **2019**, *4*, 463–478.
[12] W. H. Binder, O. W. Smrzka, *Angew. Chem. Int. Ed.* **2006**, *45*, 7324–7328; *Angew. Chem.* **2006**, *118*, 7482–7487.
[13] N. M. Sangeetha, U. Maitra, *Chem. Soc. Rev.* **2005**, *34*, 821.
[14] G. Angelici, G. Falini, H.-J. Hofmann, D. Huster, M. Monari, C. Tomasini, *Angew. Chem. Int. Ed.* **2008**, *47*, 8075–8078; *Angew. Chem.* **2008**, *120*, 8195–8198.
[15] S. Awhida, E. R. Draper, T. O. McDonald, D. J. Adams, *J. Colloid Interface Sci.* **2015**, *455*, 24–31.
[16] L. A. Estroff, A. D. Hamilton, *Chem. Rev.* **2004**, *104*, 1201–1218.
[17] X. Du, J. Zhou, J. Shi, B. Xu, *Chem. Rev.* **2015**, *115*, 13165–13307.
[18] A. M. Pisoschi, *J. Biobased Mater. Bioenergy* **2013**, *7*, 19–38.
[19] K. Prasad, D. Mondal, M. Sharma, M. G. Freire, C. Mukesh, J. Bhatt, *Carbohydr. Polym.* **2018**, *180*, 328–336.
[20] M. R. N. Monton, E. M. Forsberg, J. D. Brennan, *Chem. Mater.* **2012**, *24*, 796–811.
[21] X. Fan, C. P. Teng, J. C. C. Yeo, Z. Li, T. Wang, H. Chen, L. Jiang, X. Hou, C. He, J. Liu, *Macromol. Rapid Commun.* **2021**, *42*, 1–8.
[22] N. Singh, M. Kumar, J. F. Miravet, R. V. Ulijn, B. Escuder, *Chem. A Eur. J.* **2017**, *23*, 981–993.
[23] K. G. Cho, J. I. Lee, S. Lee, K. Hong, M. S. Kang, K. H. Lee, *Adv. Funct. Mater.* **2020**, *30*, 1907936.
[24] Y. Yao, L. Zhang, E. Orgiu, P. Samorì, *Adv. Mater.* **2019**, *31*, 1–20.
[25] A. K. Gaharwar, N. A. Peppas, A. Khademhosseini, *Biotechnol. Bioeng.* **2014**, *111*, 441–453.
[26] Y. Mu, X. Wu, D. Pei, Z. Wu, C. Zhang, D. Zhou, X. Wan, *ACS Biomater. Sci. Eng.* **2017**, *3*, 3133–3140.
[27] D. Giuri, L. Jurković, S. Fermani, D. Kralj, G. Falini, C. Tomasini, *ACS Biomater. Sci. Eng.* **2019**, *2*, 5819–5828.
[28] L. Milli, N. Zanna, A. Merlettini, M. Di Giosia, M. Calvaresi, M. L. Focarete, C. Tomasini, *Chem. A Eur. J.* **2016**, *22*, 12106–12112.
[29] D. Giuri, N. Zanna, C. Tomasini, *Gels* **2019**, *5*, 27.
[30] B. O. Okesola, D. K. Smith, *Chem. Soc. Rev.* **2016**, *45*, 4226–4251.
[31] B. Adhikari, G. Palui, A. Banerjee, *Soft Matter* **2009**, *5*, 3452–3460.
[32] G. Guidetti, D. Giuri, N. Zanna, M. Calvaresi, M. Montalti, C. Tomasini, *ACS Omega* **2018**, *3*, 8122–8128.
[33] N. Zanna, C. Tomasini, *Gels* **2017**, *3*, 39.
[34] X. Hou, L. Mu, F. Chen, X. Hu, *Environ. Sci.-Nano* **2018**, *5*, 2216–2240.
[35] F. Xiaoli, C. Qiyue, G. Weihong, Z. Yaqing, H. Chen, W. Junrong, S. Longquan, *Arch. Toxicol.* **2020**, *94*, 1915–1939.
[36] W. N. Missaoui, R. D. Arnold, B. S. Cummings, *Chem.-Biol. Interact.* **2018**, *295*, 1–12.
[37] M. Pogribna, G. Hammons, *J. Nanobiotechnol.* **2021**, *19*, DOI 10.1186/s12951-020-00740–0.
[38] F. Lu, D. Astruc, *Coord. Chem. Rev.* **2020**, *408*, 213180.
[39] A. M. Awad, R. Jalab, A. Benamor, M. S. Nasser, M. M. Ba-Abbad, M. El-Naas, A. W. Mohammad, *J. Mol. Liq.* **2020**, *301*, 112335.
[40] S. Homaeigohar, *Nanomaterials* **2020**, *10*, DOI 10.3390/nano10020295.

[41] Y. Luo, W. Guo, H. H. Ngo, L. D. Nghiem, F. I. Hai, J. Zhang, S. Liang, X. C. Wang, *Sci. Total Environ.* **2014**, *473–474*, 619–641.
[42] Y. Inai, T. Oshikawa, M. Yamashita, T. Hirabayashi, T. Hirako, *Biopolymers* **2001**, *58*, 9–19.
[43] S. K. Maji, D. Haldar, M. G. B. Drew, A. Banerjee, A. K. Das, A. Banerjee, *Tetrahedron* **2004**, *60*, 3251–3259.
[44] B. V. V. Prasad, H. Balaram, P. Balaram, *Biopolymers* **1982**, *21*, 1261–1273.
[45] G. D. Rose, L. M. Glerasch, J. A. Smith, *Adv. Protein Chem.* **1985**, *37*, 1-109.
[46] S. Panja, D. J. Adams, *Chem. Commun.* **2019**, *55*, 10154–10157.
[47] J. Rivera-Utrilla, M. Sánchez-Polo, M. Á. Ferro-García, G. Prados-Joya, R. Ocampo-Pérez, *Chemosphere* **2013**, *93*, 1268–1287.
[48] H. Guo, Z. Xu, D. Wang, S. Chen, D. Qiao, D. Wan, H. Xu, W. Yan, X. Jin, *Chemosphere* **2022**, *286*, 131580.
[49] E. Brillas, *Chemosphere* **2022**, *286*, 131849.
[50] Q. Sun, H. Zheng, X. Hu, M. Salam, M. Sun, C. Zhao, B. Bao, *Sep. Purif. Technol.* **2021**, *274*, 118694.
[51] T. Heberer, *Toxicol. Lett.* **2002**, *131*, 5–17.
[52] G. M. Sheldrick, *Acta Crystallogr. Sect. A* **2015**, 71, 3–8.
[53] G. M. Sheldrick, *Acta Crystallogr. Sect. C* **2015**, 71, 3–8.
[54] O. V. Dolomanov, L. J. Bourhis, R. J. Gildea, J. A. K. Howard, H. Puschmann, *J. Appl. Crystallogr.* **2009**, *42*, 339–341.
[55] A. Thorn, B. Dittrich, G. M. Sheldrick, *Acta Crystallogr. Sect. A* **2012**, *68*, 448–451.
[56] C. F. Macrae, I. J. Bruno, J. A. Chisholm, P. R. Edgington, P. McCabe, E. Pidcock, L. Rodriguez-Monge, R. Taylor, J. Van De Streek, P. A. Wood, *J. Appl. Crystallogr.* **2008**, *41*, 466–470.

Manuscript received: February 24, 2022
Accepted manuscript online: February 26, 2022
Version of record online: ■■, ■■■

RESEARCH ARTICLE

An aromatic-free and low-impact technology that efficiently entraps aqueous pollutants is reported. We formed gels, using the aromatic-free tripeptide Boc-L-Ala-Aib-L-Val-OH with mixtures of water and alcohols. The hydrogel formed in 2-propanol/water traps up to 97.0% of Eosin Y and up to 88.6% of Diclofenac sodium from aqueous solutions. The hydrogel is also thixotropic, thermoreversible and biocompatible.

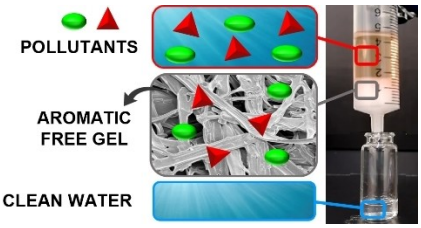

Dr. D. Giuri, Dr. S. D'Agostino, P. Ravarino, D. Faccio, Prof. G. Falini, Prof. C. Tomasini**